Low-temperature properties of CeRu$_4$Sn$_6$ from NMR and specific heat measurements: Heavy fermions emerging from a Kondo-insulating state

E. M. Brüning,[1,*] M. Brando,[1] M. Baenitz,[1] A. Bentien,[1] A. M. Strydom,[2] R. E. Walstedt,[3] and F. Steglich[1]

[1]*Max Planck Institute for Chemical Physics of Solids, Nöthnitzer Straße 40, 01187 Dresden, Germany*
[2]*Physics Department, University of Johannesburg, P.O. Box 524, Auckland Park 2006, South Africa*
[3]*Physics Department, University of Michigan, Ann Arbor, Michigan 48109, USA*

The combination of low-temperature specific heat and nuclear-magnetic-resonance (NMR) measurements reveals important information on the ground-state properties of CeRu$_4$Sn$_6$, which has been proposed as a rare example of a tetragonal Kondo insulator (KI). The NMR spin-lattice-relaxation rate $1/T_1$ deviates from the Korringa law below 100 K signaling the onset of an energy gap $\Delta E_{g1}/k_B \approx 30$ K. This gap is stable against magnetic fields up to 10 T. Below 10 K, however, unusual low-energy excitations of in-gap states are observed, which depend strongly on the field H. The specific heat C detects these excitations in the form of an enhanced Sommerfeld coefficient $\gamma = C(T)/T$: in zero field, γ increases steeply below 5 K, reaching a maximum at 0.1 K, and then saturates at $\gamma \approx 0.6$ J/K^2 mol. Upon increasing field, this maximum is shifted to higher temperatures with an overall reduction in γ, suggesting a residual density of states at the Fermi level developing a spin (pseudo-)gap ΔE_{g2}. A simple model, based on two narrow quasiparticle bands located at the Fermi level—which cross the Fermi level in zero field at 0.022 states/meV f.u.—can account qualitatively as well as quantitatively for the measured observables. In particular, it is demonstrated that fitting this model, incorporating a Ce magnetic moment of $\mu = \Delta E_{g1}/\mu_0 H \approx 1$ μ_B, to our data of both specific heat and NMR leads to the prediction of the field dependence of the gap. Our measurements rule out the presence of a quantum critical point as the origin for the enhanced γ in CeRu$_4$Sn$_6$ and suggest that this arises rather from correlated, residual in-gap states at the Fermi level. This work provides a fundamental route for future investigations into the phenomenon of narrow-gap formation in the strongly correlated class of systems.

I. INTRODUCTION

Among the wide variety of electronic and magnetic ground states played out by the variable hybridization between a local magnetic moment and degenerate conduction-electron states, the formation of a semiconducting ground state remains enigmatic. The simple picture of a single half-filled conduction-band mixing with one magnetic level per site to produce the Kondo insulating (or heavy-fermion semiconducting) state gives an appealingly simple description for this class of materials. The body of experimental evidence is not so unequivocal, however, and even the involvement of hybridization which drives the Kondo interaction and supposedly realizes a semiconducting state in theses systems, has been brought into question.

Kondo-insulator (KI) materials (e.g., see Ref. 1, and references therein) are Kondo lattice (KL) systems which exhibit semiconducting behavior below a certain temperature T_g at which an energy gap opens at the Fermi level.[2,3] Although numerous investigations have been performed on Kondo-insulator compounds, where the behavior of the gap has been observed under the effect of external parameters such as pressure[4] or magnetic field,[1] the intrinsic conditions under which a KL transforms into a KI are still not clear. A puzzling phenomenon that complicates the concept of a hybridization gap,[2] is the fact that an electrically insulating ground state as $T \rightarrow 0$ is rather uncommon. In this group of KI systems a small residual carrier concentration and hence a finite electrical conductivity for $T \rightarrow 0$ appears to be generic, as observed at low temperature.[5]

The general physical properties of CeRu$_4$Sn$_6$ are attributed to the formation of the Kondo-insulating state in this compound.[5,6] The residual carrier levels in CeRu$_4$Sn$_6$ have a magnetic origin and yet muon-spin relaxation (μSR) experiments,[7] a probe which is exceedingly sensitive to magnetic cooperation phenomena, prove the ground state of CeRu$_4$Sn$_6$ to be free from long-range or even short-range ordering. CeRu$_4$Sn$_6$ belongs to a family of rare-earth R-Ru$_4$Sn$_6$ ternary stannides.[8,9] Together with U$_2$Ru$_2$Sn, it is a rare occurrence of KI having tetragonal crystal structure (crystallographic space group $I\bar{4}2m$). Evidence of the onset of an energy gap at about 30 K has been found in the temperature dependence of several quantities: electrical resistivity (ρ) and thermal conductivity (κ),[5,6] spin-lattice-relaxation rate ($1/T_1$) in nuclear-magnetic-resonance (NMR) experiments[10] and thermopower (S).[5]

The T-dependent thermopower of CeRu$_4$Sn$_6$ and LaRu$_4$Sn$_6$ is shown in Fig. 1. It was measured in zero field and at 9 T in the temperature range between 2 and 375 K. In the measured temperature range there is no indication of peaks which can be attributed to a crystalline electric field (CEF) splitting. This is consistent with inelastic neutron-scattering experiments[11] from which a resonance of magnetic origin at about 30 meV $\approx$ 350 K is the only evidence of CEF effects in CeRu$_4$Sn$_6$ in this temperature range. For LaRu$_4$Sn$_6$ (zero field), S shows a linear temperature dependence for $T \rightarrow 0$ which is characteristic of simple metals.[12] In fact, S can be obtained from the thermoelectric potential by applying a temperature gradient, and in metals $S(T)$ com-
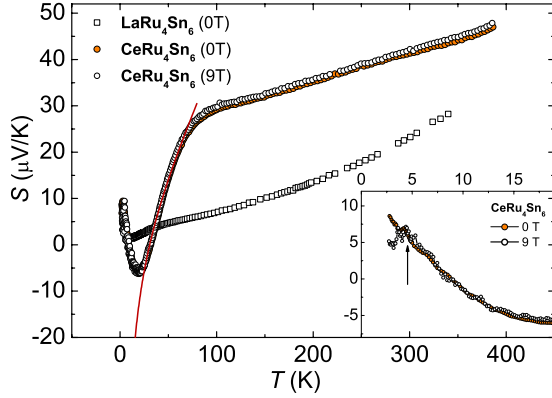
FIG. 1. (Color online) Temperature dependence of the thermopower measured in 0 and 9 T. The line shows a fit according to an energy-gap-derived contribution $S(T)_{gap} \propto \Delta E_{g1}/k_B T$ (see text). Inset: low-temperature $S(T)$ data at 0 and 9 T. The arrow indicates the maximum observed at 9 T.

monly tracks the energy derivative of the electronic density of states $N(E)$ at the Fermi energy,

$$S \propto T \left[\frac{\partial \ln N(E)}{\partial E} \right]_{E=E_F}. \tag{1}$$

In a rigid band model, where $N(E)$ is temperature independent, S is therefore proportional to T. A linear-T relation can also be observed in the thermopower of $CeRu_4Sn_6$ above $T = 100$ K, even though the absolute values are enhanced, compared to those of $LaRu_4Sn_6$. Above 50 K, the thermopower can be ascribed to a conduction band in a semimetal.[12] Here, $S(T)$ can be expressed as a sum of a contribution $S_0 \propto T$ and a contribution $S_{gap}(T) \propto \Delta E_{g1}/k_B T (\Delta E_{g1}/k_B = 36$ K) (Ref. [5]) (line in Fig. [1]). The size of the energy gap is consistent with that found in resistivity measurements.[6] Toward lower temperatures, $S(T)$ strongly decreases and reaches a maximum negative value at $T \simeq 22$ K. This is characteristic of correlated semimetals with a residual density of states within an energy gap, as is also found, for example, in the Kondo insulator SmB_6.[13] At temperatures lower than the 22 K extremum, $S(T)$ turns toward $S=0$ which is achieved near 8 K, but further cooling sees an increase in S toward positive values. Since the third law of thermodynamics predicts $S=0$ at $T=0$, a maximum in $S(T)$ is expected toward lower temperatures.[14] The temperature range between 2 and 15 K is shown in the inset of Fig. [1]. Here, an applied field of $\mu_0 H = 9$ T shifts the maximum expected at low T in $S(T)$ to around 5 K and indeed projects the thermopower back toward zero as $T \rightarrow 0$. This observed field dependence likely suggests further low-lying phenomena such as a small gapped structure within the narrow f band. The sensitive nature of $S(T)$ to fields is in accord with the magnetic nature of the in-gap states. This interpretation is also supportive of former heat-capacity results performed in magnetic field for temperatures larger than 0.3 K, where a maximum is observed in C/T vs T which shifts to higher temperatures with increasing H.[5]
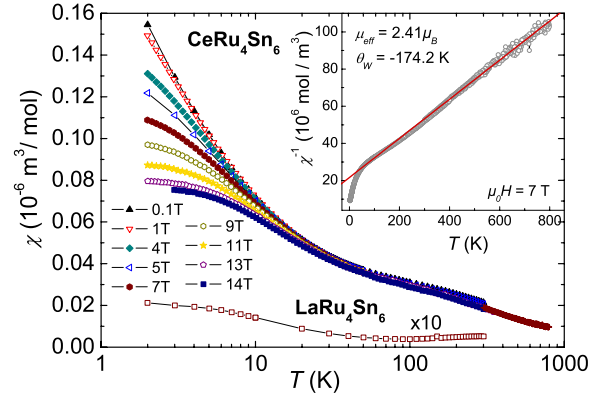

FIG. 2. (Color online) Magnetic susceptibility of $CeRu_4Sn_6$ in a semilog scale, showing the field dependence that develops below 20 K (main panel) and the local-moment magnetic character inferred from the high-temperature data (inset). For comparison, the very small and weakly temperature-dependent χ of nonmagnetic $LaRu_4Sn_6$ is also shown.

The concept of magnetic residual in-gap states is proven by the uniform susceptibility $\chi(T,H)=M(T)/H$ shown in Fig. [2]. The results portray the paramagnetic state with a strong field dependence of the susceptibility developing below 20 K. The inverse susceptibility follows a Curie-Weiss law down to 50 K, without any sign of CEF splitting. From the slope we determine an effective moment of $\mu_{eff} = 2.41$ μ_B/Ce which is close to the free Ce^{3+} moment ($\mu_{eff} = 2.54$ μ_B/Ce), indicating a well localized Ce moment at high temperatures. Below 50 K, a strong deviation from the Curie-Weiss law is observed and it is associated with the opening of a gap. Considering the involvement of Kondo physics in $CeRu_4Sn_6$,[5] a partial compensation of the local moments due to on-site moment screening may also be involved in the temperature evolution of $\chi(T)$ at intermediate temperatures. However, in the observed $\chi(T)$ of $CeRu_4Sn_6$ the opening of the energy gap at about 30 K does not appear to cause the typical KI-like *decrease* in $\chi(T)$ below a gap-derived maximum. In the KI class of systems, this feature originates from the stable local-moment susceptibility at high temperatures which turns into a demagnetized state at low temperature through severe hybridization with the degenerate conduction-band states. In the present case we rather observe an increase in $\chi(T)$ toward low temperatures. On cooling, no significant field dependence of χ could be resolved down to 20 K. Below this temperature the behavior changes. With increasing magnetic field the susceptibility tends to level off at a small constant value as is visible in the 14 T curve. This behavior confirms the presence of a residual density of states within an energy gap. In contrast to that, the structural homolog $LaRu_4Sn_6$ shows a nearly temperature-independent Pauli susceptibility as it is expected for a nonmagnetic metal.

The partial density of states accessible to a magnetic field at 2 K can be also seen in the field dependence of the magnetization M, shown in Fig. [3]. At 2 K and 14 T a value of only $M \simeq 0.2$ μ_B/Ce is reached which corresponds to only about 9.3% of the full gJ complement of the Ce^{3+} moment. Consequently, no saturation could be observed up to 14 T.
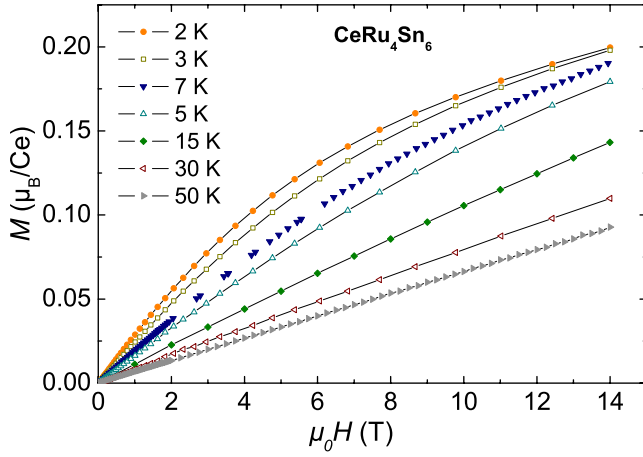
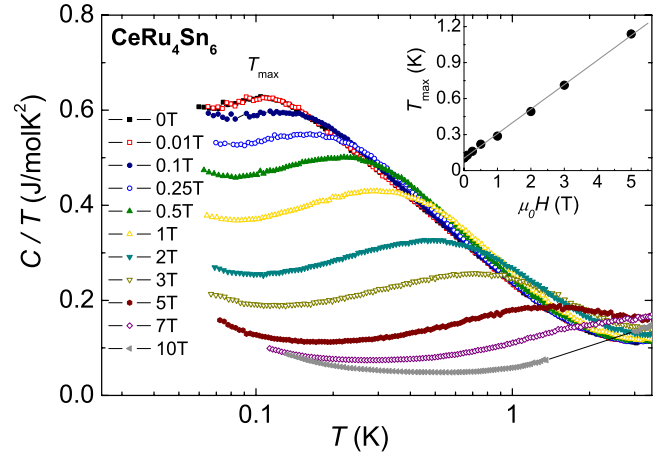FIG. 3. (Color online) Magnetization isotherms of CeRu$_4$Sn$_6$.

FIG. 4. (Color online) Sequence of isofield plots of the low-temperature specific heat of CeRu$_4$Sn$_6$. Inset: field variation in the temperature T_{max} where a maximum is achieved in $C(T,H)$, after subtraction of the nuclear contributions, see text.

In this paper, we focus essentially on the low-temperature properties of CeRu$_4$Sn$_6$ for which the opening of the 30 K energy gap is a key ingredient. We demonstrate how two strongly correlated (narrow) quasiparticle bands, located at the Fermi level, can account qualitatively and quantitatively for all properties observed in this material. Although rather exotic, it is our contention that the scenario played out in the ground state of CeRu$_4$Sn$_6$ has features which make the proposed model more generally applicable to similar systems in the class of correlated materials.

II. EXPERIMENTAL

All measurements shown in this paper have been carried out on sample material originating from the same batch. The polycrystalline sample was synthesized in an arc furnace followed by subsequent phase purifying heat treatment. The details of the preparation are reported elsewhere.[5] Physical properties, magnetization, and thermopower measurements were carried out in a standard Quantum Design Physical Property Measurement System (PPMS) and Magnetic Property Measurement System (MPMS) in the temperature range from 1.8 to 300 K. The MPMS high-temperature option was used for magnetization measurements up to 800 K. NMR measurements were obtained in a temperature range between 2 and 250 K in a ^{4}He cryostat (Janis) and with a commercial pulsed NMR spectrometer (TecMag) using the field-sweep method. The field-sweep NMR measurements were performed with different fields and frequencies, respectively. For the spin-lattice-relaxation measurements, a saturation-recovery sequence was applied. The heat capacity has been measured in a dilution refrigerator with the compensated heat-pulse method[15] from 4 K down to 0.065 K and in static applied fields up to 10 T.

III. RESULTS

A. Specific heat

Field-dependent investigations of the specific heat $C(T)$ of LaRu$_4$Sn$_6$ and CeRu$_4$Sn$_6$ in the temperature range between 0.4 and 20 K have been reported in Ref. 5. In zero field, a logarithmic increase in the Sommerfeld coefficient $\gamma = C/T$ versus T (extended, on cooling, over a decade in temperature) has been observed. Non-Fermi-liquid behavior such as this, similar to what is often seen in strongly correlated systems, for instance, in proximity to a continuous quantum phase transition, has been a subject of considerable interest. In CeRu$_4$Sn$_6$ this particular aspect of the ground state has been addressed using μSR studies which portrayed an interpretation in terms of low-temperature quantum fluctuations.[7]

Detailed low-temperature specific heat results are shown in Fig. 4. In the whole temperature range, no sign of a phase transition, e.g., magnetic ordering or superconductivity, could be found, in good agreement with μSR measurements.[7] At the lowest temperatures a weak increase in C/T with decreasing T is attributed to a nuclear Schottky contribution. At temperatures sufficiently larger relative to the nuclear splitting energy, the high-temperature tail of a Schottky excitation is expected which should follow $C \sim 1/T^2$. In the present case, such a contribution likely arises from ^{119}Sn and ^{117}Sn isotopes and ^{99}Ru and ^{101}Ru isotopes. The nuclear Schottky contribution furthermore commonly scales with the magnetic field as H^2, as it does in our case. This low-temperature nuclear contribution is subtracted (for the analysis performed in Sec. III C.) and is of no further consequence to the interpretation of our data.

As seen in Fig. 4, a local maximum develops at T_{max} =0.1 K which shifts toward higher temperatures with increasing field. In the inset of Fig. 4, T_{max} vs $\mu_0 H$ is plotted and a well-defined linear-in-H dependence of T_{max} is observed, hinting at Zeeman splitting of degenerate spin states by the applied magnetic field[16] (p. 143).

From these measurements we can now conclude that (i) the behavior of $\gamma(T)$ below 5 K is not related to the presence of a quantum phase transition, but is probably a consequence of correlated in-gap states, and (ii) a presumed degeneracy is lifted in applied magnetic fields, causing a maximum in $\gamma(T)$.
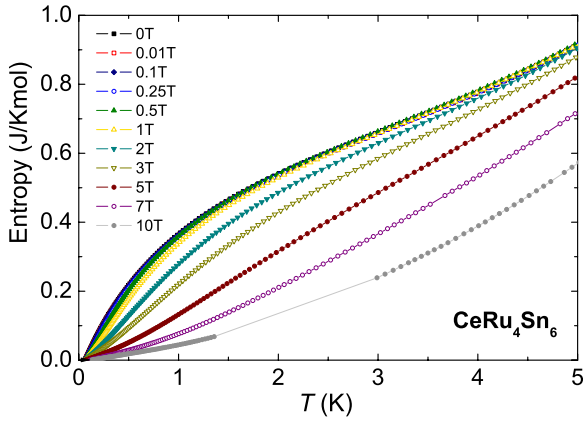
FIG. 5. (Color online) Temperature-dependent entropy of $CeRu_4Sn_6$ obtained at various fields up to 10 T.

B. Remarks about the entropy

The tetragonal crystal structure of $CeRu_4Sn_6$ would imply a CEF-derived Kramers doublet as a ground state for the magnetic Ce^{3+} ion with an entropy contribution of $R \ln 2$ = 5.76 J/mol K. In the absence of significant CEF splitting, deduced from our thermopower and susceptibility measurements above $T \approx \Delta E_{g1}/k_B = 30$ K up to 800 K, one may expect the entropy of the non-degenerate $J = 5/2$ state of Ce^{3+}, $R \ln 6$, to be quenched below 30 K where the gap opens and the Kondo effect starts to screen the Ce moments. However, in inelastic neutron-scattering experiments a q-independent peak at about 30 meV ≈ 350 K has been detected which likely signals a high-lying CEF-derived doublet.[17] This could explain the small discrepancy between the effective moment found in the susceptibility (cf. Fig. 2) and that of the full Ce^{3+} free-ion moment. Nonetheless, this still leaves a magnetic entropy amounting to $R \ln 4$ for the ground state. The entropy of $CeRu_4Sn_6$, after having subtracted the nuclear but not the phonon contribution, is plotted in Fig. 5: surprisingly, at 5 K, less than 10% of $R \ln 4$ is recovered in zero field. Applied magnetic fields shift the entropy toward higher temperatures. We performed high-resolution measurements of two nonmagnetic isostructural compounds, $LaRu_4Sn_6$ and YRu_4Sn_6, with a view to subtracting the phononic contribution and check how much magnetic entropy is recovered at 30 K. However, as was mentioned in Ref. 5, caution has to be exercised in this procedure and the La compound may not be considered as a proper phononic analog for the Ce one in this class of materials. A similar conclusion was drawn, for instance, on the KI CeRhSn.[18] There are two main reasons for that: (i) the nonmagnetic compounds $LaRu_4Sn_6$ and YRu_4Sn_6 are metallic at low temperature whereas $CeRu_4Sn_6$ is not, and (ii) all these materials form in a so-called cage structure which exhibits not only acoustic-phonon modes but also optical ones due to the anharmonic motion of caged-up atoms in the cage framework. The Einstein frequencies of these modes depend on the lattice constants, and they will give generally different contributions to the specific heats of $LaRu_4Sn_6$ and $CeRu_4Sn_6$. Indeed, the measured $C(T)$ curves of $CeRu_4Sn_6$ and $LaRu_4Sn_6$ (or YRu_4Sn_6) were found to cross each other below 10 K. Attempts to subtract the elec-

tronic specific heat of $LaRu_4Sn_6$ from that of $CeRu_4Sn_6$ were inconclusive for understanding at which temperature at least an amount of entropy close to $R \ln 2$ is recovered. Since the Ce magnetic moment at 0.06 K is small and thus only a tiny amount of entropy is left to be released below this temperature, it follows that at least 80% of $R \ln 2$ has to be distributed between 5 and 30 K, in agreement with the assumption that around 30 K a gap opens.

Considering NMR as a sensitive microscopic probe for the formation of an energy gap, as well as the involvement of correlated states and their evolution in a magnetic field, we proceed to describe in the next section our ^{119}Sn-NMR results.

C. ^{119}Sn NMR spectroscopy

To investigate the low-energy excitations, we have chosen Sn-NMR as microscopic probe. Particularly, we selected the ^{119}Sn isotope (nuclear spin $I = 1/2$) which exhibits the highest natural abundance (8.58%) among the three isotopes. This allows for a good NMR signal. In general, NMR can provide information about the existence of an energy gap and its shape. In relation to studies on KIs especially, detailed NMR studies on systems such as CeNiSn,[19,20] $Ce_3Bi_4Pt_3$,[21] SmB_6,[22] and U_2Ru_2Sn (Ref. 23) have been shown to benefit from the acute sensitivity of NMR response to changes in the charge-carrier density of states and narrow gap formation. The spectra of the $CeRu_4Sn_6$ polycrystals were obtained with the field-sweep method at 47 MHz (Fig. 6, top panel). Due to the two inequivalent sites occupied by Sn in the unit cell, the NMR spectrum exhibits two lines with an ideal intensity ratio of 2:1. Therefore, the powder pattern consists of a superposition of two anisotropic Sn1 and Sn2 lines.

This is emphasized for a single spectrum at 10 K in Fig. 6 (middle panel). The well-defined line shape suggests that the sample is homogeneous and no disorder effects are evident. To determine the Larmor field H_L ($K_{iso} = 0$), the reference material α-SnO with $^{119}K_{iso} = 0.5\%$ was used[24] (dashed-dotted vertical line in Fig. 6). It follows that the isotropic NMR shift of the ^{119}Sn spectra of $CeRu_4Sn_6$ is very small ($^{119}K_{iso} \simeq 0.5\%$) and nearly temperature independent. In contrast, the ^{119}Sn-NMR spectra of the structurally related stannides $CeRuSn_3$ and $Ce_3Ru_4Sn_{13}$, both of which are classified as heavy-fermion metals,[25,26] exhibit larger and temperature-dependent shifts ($^{119}K \simeq 4\%$) at 4 K. The small shift in $CeRu_4Sn_6$ reflects a weak hyperfine coupling because of the low carrier density.

The spectra of $LaRu_4Sn_6$ show a Gaussian broadening and only a weak anisotropy (see Fig. 6, bottom panel). $LaRu_4Sn_6$ is a good metal and a weak Pauli paramagnet. A negative shift in this case might be attributed to a chemical shift. At higher temperatures ($130 < T \leq 250$ K), the ^{119}Sn-NMR spectra of $CeRu_4Sn_6$ show two distinct maxima which are attributed to the two Sn positions $K_{\perp}$. Toward lower temperatures, the spectra broaden and the two sharp maxima can no longer be easily resolved. The anisotropic shift of the two Sn lines attributed to the spectral overlap of the two inequivalent Sn sites imparts an arbitrary element to their simulation which makes a quantitative analysis of these
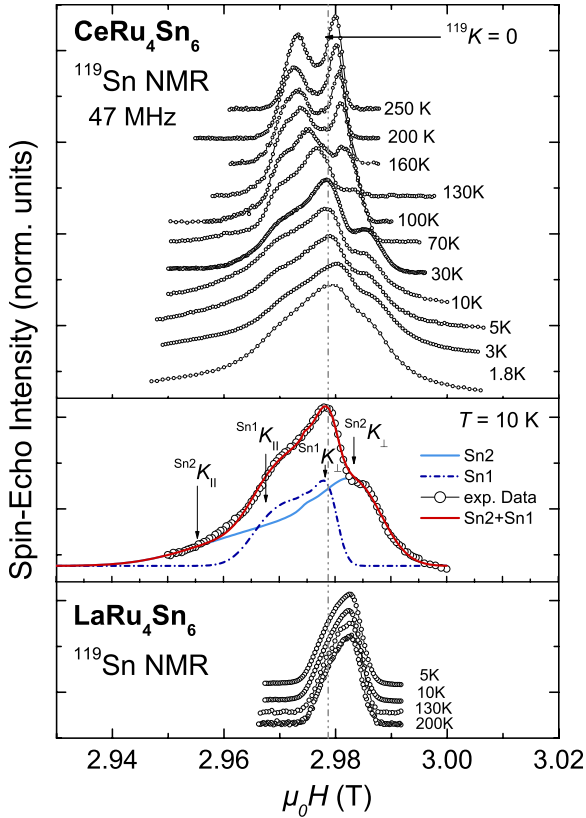
FIG. 6. (Color online) Field-dependent ^{119}Sn-NMR spectra obtained at various sample temperatures. By comparison, the nonmagnetic homolog LaRu$_4$Sn$_6$ produces an NMR response (bottom panel) with no discernible temperature variation. The middle panel shows a simulation of the spectra associated with the two inequivalent Sn sites and the resulting spectrum; $K_\perp$ and $K_\parallel$ denote the local maxima attributed to the shift perpendicular and parallel to the c axis, respectively.

spectra rather tenuous. Therefore, we limit our interpretation to what can be learnt from estimating the NMR shift and the hyperfine field.

The respective frequency- and field-dependent investigations of the NMR spectra, concerning shift and broadening, should give information about the unusual behavior of the susceptibility at low temperatures ($T<10$ K). We measured field-sweep ^{119}Sn-NMR spectra at different frequencies and at two different temperatures, 30 and 5 K: the results are shown in Fig. 7. At $T=30$ K, the distribution of frequencies is caused entirely by the distribution of NMR shifts (Fig. 7, top panel) where field scans are plotted as shift distributions $(H-H_{max})/H_L$ for a range of NMR frequencies. The uniformity of shape and broadening is seen to be quite precise. When scans taken at 5 K are plotted in the same fashion (Fig. 7, bottom panel), a striking change is seen to take place. A progressively larger (fractional) broadening occurs as the frequency is lowered so that at 11 MHz the spectrum is nearly twice as wide as at 119 MHz. The analysis of the entire series of spectra can be represented by a distribution of shifts broadened by a convolution with a Gaussian function having a fixed width parameter of $H=15$ Oe. Broadening fields which are independent of the applied field only occur in
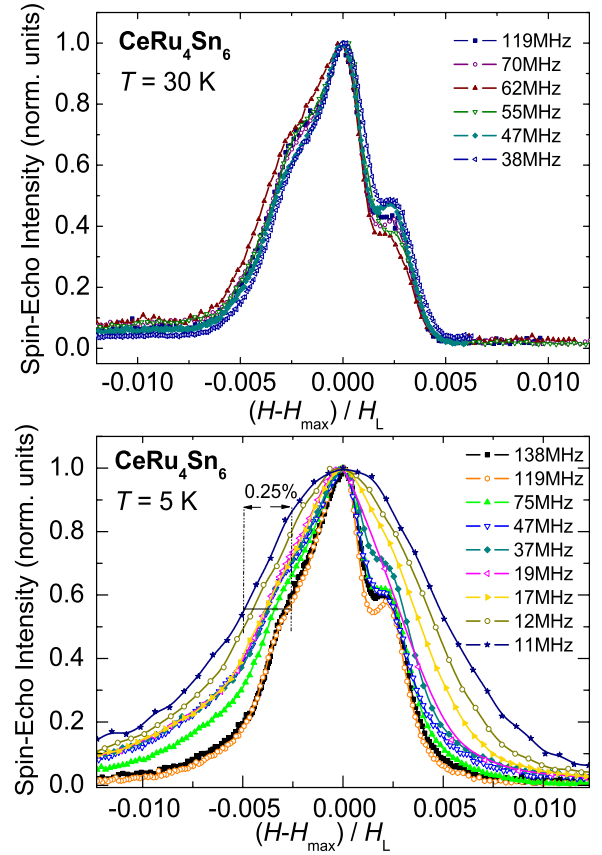

FIG. 7. (Color online) ^{119}Sn-NMR spectra at various frequencies grouped by temperature to emphasize the line broadening occurring at low temperatures. The comparatively small shift (see Fig. 6) has been normalized out.

cases of "spin freezing," e.g., in a spin glass such as Cu:Mn.[27] Thus, the field-independent broadening effect observed here corresponds to a quasistatic component in the magnetic moments. For CeRu$_4$Sn$_6$, on the contrary, no spin-glass behavior has been reported for $T>0.1$ K: there is no cusp in the ac susceptibility taken at small fields. Additionally, very slowly fluctuating moments were detected by μSR down to 0.05 K,[7] without any "freezing" of magnetic moments. The spin-lattice-relaxation time was measured with a saturation-recovery sequence at 47, 70, 100, and 119 MHz.

The investigation was carried out at the spectral maximum which corresponds to the $^{Sn1}K_\perp$ position labeled in the powder pattern plotted in Fig. 6. Due to the overlap of the NMR signal of the two Sn positions, T_1 is composed of the contributions attributed to the two Sn positions. Therefore, the recovery magnetization $M(t)$ obtained from the measurements contains contributions from both $H\perp c$ and $H\parallel c$ directions and could not be described by a simple exponential behavior, $\propto[1-\exp(-t/T_1)]$. Here, $M(t)$ could be fitted well by a stretched exponential function,

$$M(t) = M_0\left[1 - \exp\left(-\frac{t}{T_1}\right)^n\right], \tag{2}$$

where $n=0.5$ is a constant weighting factor. The data of $^{119}(1/T_1)$ extracted here should be treated as being powder
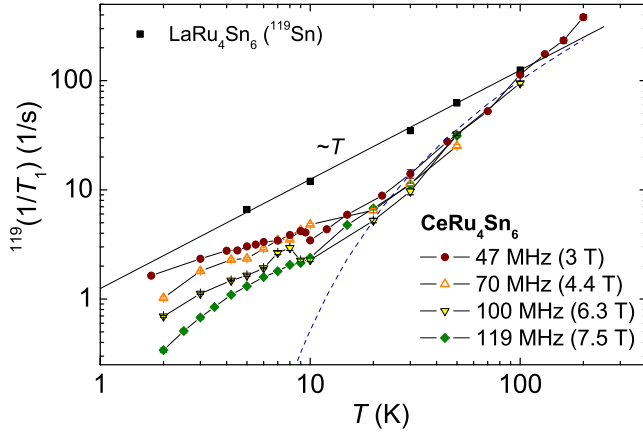
FIG. 8. (Color online) Temperature evolution of the spin-lattice-relaxation rate $^{119}(1/T_1)$ of CeRu$_4$Sn$_6$ in a double-logarithmic plot. (Dashed line: fit of an exponential function, for details see text.) For comparison, the $1/T_1 \propto T$ dependence of the reference LaRu$_4$Sn$_6$ is also shown.

averaged. The spin-lattice-relaxation rate $^{119}(1/T_1)$ is shown as a function of temperature in Fig. 8. Below 300 K down to $T \simeq 30$ K, no significant field nor frequency dependence is detected, in contrast to the situation at lower temperatures where, $^{119}(1/T_1)$ decreases with increasing field. $^{119}(1/T_1)$ of the nonmagnetic homolog LaRu$_4$Sn$_6$ is plotted in the same figure: the temperature dependence is linear as expected from the Korringa relation $1/T_1 \propto T$ for a paramagnetic metal. $^{119}(1/T_1)$ vs T of CeRu$_4$Sn$_6$ deviates significantly from that of the reference system compound LaRu$_4$Sn$_6$ toward lower temperatures. This is characteristic of systems exhibiting the opening of an energy gap at the Fermi level. This phenomenon is evident in many other KIs such as U$_2$Ru$_2$Sn,[23] CeNiSn,[19,20] Ce$_3$Bi$_4$Pt$_3$,[21] FeSb$_2$,[28] and SmB$_6$.[22,29] For noncubic systems such as CeNiSn and U$_2$Ru$_2$Sn, a T^3 power law valid over two decades in temperature was found in $^{119}(1/T_1)$ vs T. A consistent description in the entire temperature range was possible by applying the so-called V-shaped gap model for $N(E)$.[20,23] For the cubic system Ce$_3$Bi$_4$Pt$_3$ a rectangular gap with a small amount of in-gap states was used to describe $1/T_1(T)$.[21] For CeRu$_4$Sn$_6$ a T^3 power-law behavior could not be observed. Here, the existence of an energy gap ΔE_{g1} can be verified quantitatively by fitting the experimental data above approximately 10 K with $1/T_1 \propto T N^2(E_F) \propto T \exp(-\Delta E_{g1}/k_B T)$ according to the Korringa relation, which gives in our case $\Delta E_{g1} = 30$ K (dashed line in Fig. 8). This value is in good agreement with resistivity[6] and thermopower[5] results. The deduced magnitude of the energy gap seems not to be strongly dependent on the NMR magnetic field and frequency used in our experiments. It is important to note that the fit is found not to follow the $1/T_1$ vs T results over the entire temperature range, which is due to the crossover to a different power law toward lower temperatures.

Below $T \simeq 10$ K, the spin-lattice-relaxation rate deviates from the exponential behavior and becomes strongly field dependent. This field dependence of $T_1(T)$ is a rare feature. Nonetheless, similar results have been found for the ^{11}B-NMR in the Kondo insulator SmB$_6$.[22] This has been at-

TABLE I. Parameters resulting from fitting the spin-lattice-relaxation rate versus temperature with Eq. (3).

ν (MHz)	$\mu_0 H$ (T)	$\Delta E_{g2}/k_B$ (K)
47	2.96	2.23
70	4.41	3.37
100	6.30	4.86
119	7.40	5.34

tributed to low-energy excitations of magnetic states within the energy gap at the Fermi level. The origin of these states is still puzzling and controversial. In intermetallic compounds it is quite natural to invoke the extrinsic involvement of chemical impurities as opposed to more intrinsic origins. An objective view requires extrinsic defects to be considered as a possible origin for in-gap states. Intrinsic donor states with a chemical origin and surface states derived from the discontinuity of the bulk periodic potential are features implicated even in the very clean limit of semiconducting charge transport and may thus be deemed as intrinsic origins of in-gap states. The comparatively narrow NMR line shape is indicative of a good sample quality. Additionally, the μSR spectra[7] were found to accurately follow simple, one-component exponential time decays, which are evidence of a homogeneous crystal environment in the vicinity of the muon-stopping site. Thus motivated by the high-quality sample material we took a closer look at the temperature and field dependences of $1/T_1$ below 10 K. Arranging the data in an Arrhenius plot of $\log(1/T_1)$ vs $1/T$, we notice that in the low-temperature region ($1/T > 0.1$ K^{-1}), $\log(1/T_1)$ is linear in $1/T$ for all frequencies. This range can be fitted with $1/T_1(T) \propto \exp(-\Delta E_{g2}/k_B T)$, where the small gap feature $\Delta E_{g2}/k_B T$ turns out to be strongly field dependent (cf. Table I). Such a simple Arrhenius type of exponential behavior is usually found in narrow spin-gap materials such as organic spin-Peierls compounds.[30] The whole temperature range can be well described by a two-gap equation,

$$1/T_1 = aT \exp\left(-\frac{\Delta E_{g1}}{k_B T}\right) + b \exp\left(-\frac{\Delta E_{g2}}{k_B T}\right) \quad (3)$$

with a fixed value of $\Delta E_{g1} = 30$ K. The quantities a and b are adjustable parameters. The nature of the results obtained, i.e., $\Delta E_{g1} \simeq 10 \cdot \Delta E_{g2}$, imparts confidence as to the additivity of the two exponentials in Eq. (3). The least-squares fits of the function in Eq. (3) are shown as solid lines in Fig. 9. This function describes the experimental data quite well and provides a basis from which to consider a two-gap scenario in CeRu$_4$Sn$_6$. The ΔE_{g2} values are summarized in Table I. This result suggests that a residual density of states, $N(E_F)$, exists at the Fermi level and develops an energy gap ΔE_{g2} at E_F which widens with increasing magnetic field. Measurements other than NMR are supportive of this description of the physics in CeRu$_4$Sn$_6$: (i) resistivity data show a saturation at low T, which suggest that a residual number of carriers exist and participate in the electronic transport;[6] (ii) in the thermopower measurements, a maximum in $S(T)$ is found at T
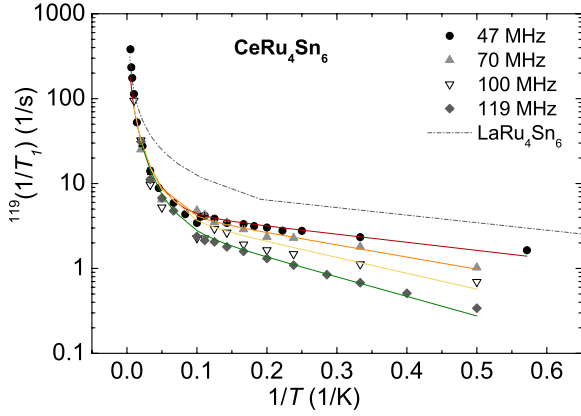
FIG. 9. (Color online) Arrhenius plot of the spin-lattice-relaxation rate to emphasize the two-gap origin of the temperature behavior [see Eq. (3)]. The solid lines correspond to the results of a calculation in the frame of a two-gap model (for details see text).

$\simeq 3$ K (zero field) which is shifted at 9 T to $T \simeq 5$ K (Fig. 1); (iii) the Sommerfeld coefficient shows a maximum in zero field which moves toward higher temperatures with field as well (Fig. 4); and (iv) the Sommerfeld coefficient in zero field is strongly enhanced indicating the existence of electronic quasiparticles with large effective masses.

D. Low-temperature specific heat and narrow-band model

Since the specific heat is directly linked to the density of states at the Fermi level through

$$C = \frac{dU}{dT} = \int_{-\infty}^{+\infty} E N(E) \frac{df(E)}{dT} dE, \qquad (4)$$

where U is the free energy and $f(E)$ the Fermi function,[31] we have analyzed $C(T)/T$ assuming for the density of states two narrow bands represented by a Cauchy-Lorentz function,

$$N(E) = z \times \frac{1}{2\pi} \left[\frac{\Gamma}{(E - \Delta)^2 + \Gamma^2} + \frac{\Gamma}{(E + \Delta)^2 + \Gamma^2} \right]. \qquad (5)$$

The quantity Δ denotes the energy gap ΔE_{g2}, Γ is the full width at half maximum and the parameter z is a weighting factor. A plot of this function is illustrated in Fig. 10.

The density of states considered here represents only the in-gap states by means of the trial function since the real density of states cannot be determined exactly with the data at hand. In the following, we discuss the application of this function and the adherence of the calculated curve to the measured data.

It is shown in Fig. 11 that a gapped band structure and the density-of-states enumeration accurately describes specific heat and NMR results in a consistent manner. To fit the specific heat data at all fields with just three parameters (Δ, Γ, and z), the nuclear Schottky contribution was subtracted and the high-temperature range was considered field independent with a Sommerfeld coefficient of 0.08 J/mol K^2 and a phonon contribution with a Debye temperature of $\Theta_D = 250$ K. The phenomenological description accounts for the T- and H-dependent specific heat data surprisingly well. The param-
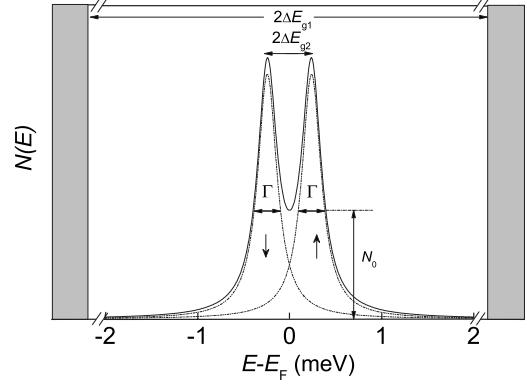

FIG. 10. Model of the residual field-dependent states in the large hybridization gap ΔE_{g1}. This model was used for the calculation of $C(T,H)$ and $T_1^{-1}(T,H)$ of CeRu$_4$Sn$_6$. Please note that the free parameters Δ, Γ, and z are field dependent and temperature independent. Values used for the calculation are listed in Table II; Fig. 12 shows the resulting field-dependent plots of $N(E)$.

eters used to fit the data are listed in Table II, and a graphical representation is illustrated in Fig. 12. To check the validity of the model, we have used the same $N(E)$ functions to calculate the spin-lattice-relaxation rate, because it can be described by[3]

$$1/T_1 \propto H_{hf}^2 \int N^2(E) f(E) [1 - f(E)] dE, \qquad (6)$$

where the only adjustable parameter is the hyperfine field H_{hf}, the role of which is only to shift up and down the fitting curves of an Arrhenius plot. The slope of these lines is given by the size of Δ. The results are shown in the inset of Fig. 11 for three different magnetic fields and these fits describe the experimental data very reliably.

The change in the density of states with increasing magnetic field is shown in Fig. 12 and the behavior reminds one of the $s = 1/2$ Kondo impurity model.[32] The shallow peak in the zero-field data of $C(T)/T$ at $T = 0.1$ K or the resulting shallow pseudogap in the $H = 0$ $N(E)$ dependence of the
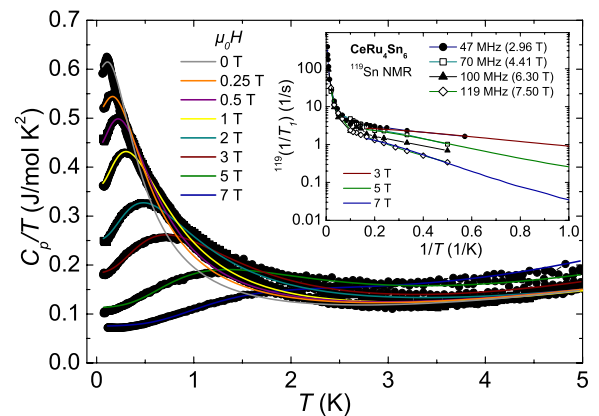

FIG. 11. (Color online) Temperature dependence of the specific heat (main panel) and spin-lattice-relaxation rate (inset) together with fits for each applied field, according to Eqs. (4)–(6), respectively.

TABLE II. List of the parameters used to fit $C(T)/T$ vs T with the density of states of the form given in Eq. (5). The X^2 parameter indicates the adherence of the fits.

μ_0H (T)	Δ (meV)	Γ (meV)	z	X^2 (10^{-5})
0	0.056	0.068	12.8	20
0.25	0.073	0.079	11.9	7
0.5	0.088	0.080	11.8	5.7
1	0.113	0.090	11.4	5
2	0.168	0.110	12.0	5
3	0.240	0.138	10.9	2
5	0.400	0.140	13.5	3
7	0.560	0.120	18	2

Fermi level suggest some static internal field to develop at the Ce sites perhaps due to spin-glass freezing although no much fields had been observed at the muon-stopping sites in μSR experiments down to $T=0.05$ K.[7] Low-temperature ac-susceptibility measurements are in preparation to clarify this point. We can now use this density of states to calculate all the observables. The point N_0 where $N(E)$ crosses the Fermi level provides the Sommerfeld coefficient $\gamma(0)$ at $T=0$. Plotting N_0 as a function of $\log(\mu_0H)$ indicates how γ decreases in an exponential fashion with increasing magnetic field [see inset (a) of Fig. 12]. To compare the values of $\Delta E_{g2}/k_BT$ obtained from NMR measurements and those obtained by fitting the specific heat data, we plotted both in the same diagram in inset (b) of the same figure. Similar values and a comparable field dependence is found among the two approaches. Assuming a Zeeman energy $\Delta E = -\vec{\mu} \cdot \vec{B}$, the magnetic moment of these states can be estimated from the slope of the dashed line in inset (b) of Fig. 12: the fit gives a value close to 1 μ_B. To estimate the number of states per formula unit, $N(E)$ can be integrated. At zero field and $T=2$ K, 0.039 states per formula unit are obtained. This value is in good accordance with that obtained from Hall-coefficient data,
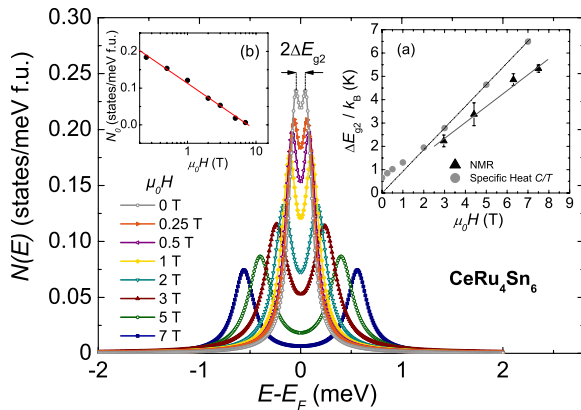
FIG. 12. (Color online) Density of states projection by means of Eq. (5) against energy relative to the Fermi energy E_F. The field-derived $T \to 0$ states density is depicted in inset (b) and inset (a) plots the field evolution of the inner gap ΔE_{g2} responsible for the low-energy properties. Lines are guides to the eye.
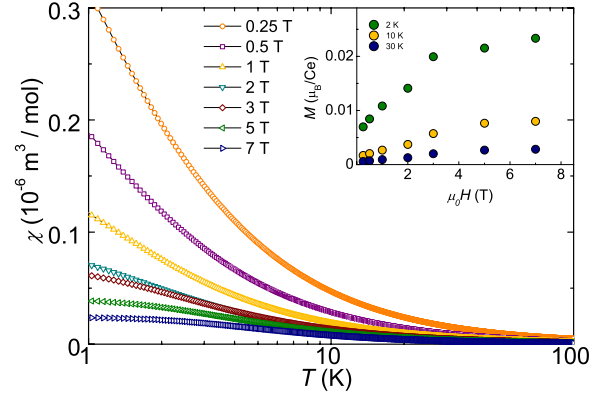
FIG. 13. (Color online) Calculated susceptibility (main panel) and magnetization (inset) guided by the density-of-states calculation of Eq. (5).

which gave 0.03 carriers per formula unit.[5] Additionally, the contribution of these spin states to the magnetization can be calculated at given values of temperature and field. Considering that the states have $s=1/2$, the magnetization can be calculated by

$$M = \mu_B(n_\uparrow - n_\downarrow), \qquad (7)$$

where

$$n_\uparrow = \frac{1}{2}\int_{-\infty}^{+\infty} N(E + \mu_B H)f(E)dE \qquad (8)$$

and

$$n_\downarrow = \frac{1}{2}\int_{-\infty}^{+\infty} N(E - \mu_B H)f(E)dE. \qquad (9)$$

For example, at $\mu_0H=7$ T and $T=2$ K, $(n_\uparrow - n_\downarrow) \simeq 0.025$ states are obtained, which cause a net magnetization $M \simeq 0.025$ μ_B/f.u. The experimental measurements (Fig. 3) yield $M \simeq 0.14$ μ_B/f.u. at the same values of temperature and field; this means that only 20% of the residual density of states contribute to the complete magnetization, where the Van Vleck contribution to M has, however, not been taken into account. The field dependence of the magnetization due to the in-gap states only is shown in the inset of Fig. 13 and is found very similar to the total magnetization in Fig. 3.

The model for the density of states [Eq. (5)] could also be successfully applied to calculate the complete temperature and field dependences of the susceptibility. This calculation for selected fields is illustrated in Fig. 13. Qualitatively, the steep increase in $\chi(T)$ at low temperatures can be reproduced by such a form of the residual density of states. Below 2 K, $\chi(T)$ flattens and its value at $T=0$ decreases with increasing field, scaling with $\gamma(0)$. The predicted trend is largely played out by the experimental results in Fig. 2. However, the absolute values differ generally from the experimental ones. It should be noted that additional effects such as an underlying magnetocrystalline anisotropy precludes a quantitative treatment in the present study on polycrystalline samples.

IV. SUMMARY AND CONCLUSIONS

We have presented detailed measurements of the field response of both the specific heat (C) and the NMR on the intermetallic Kondo-insulator compound CeRu$_4$Sn$_6$. A survey of earlier results of the electrical resistivity, thermopower, and specific heat hinted at the possibility that this system might be on the verge of magnetic order so that magnetic correlations would play an influential role in the anomalous ground-state properties. The main result of the present work is to show that strong correlations form out of a low charge carrier density which is a rare occurrence in the class of highly correlated systems. The aim of our study was to seek a description that would consistently explain the strongly enhanced low-temperature specific heat and magnetic phenomena found through NMR measurements in CeRu$_4$Sn$_6$. A V-shaped pseudogap with a broad band of residual states at the Fermi energy was first proposed by Kyogaku *et al.*[19] and provides a scenario for modeling susceptibility, Knight shift, and spin-lattice-relaxation rate in noncubic Kondo insulators such as CeNiSn and U$_2$Ru$_2$Sn. For CeRu$_4$Sn$_6$, this model is not valid, and we have assumed a simple, rigid rectangular gap model and have replaced the broad band by a narrow one of (field-dependent) residual states. We have applied this density-of-states model with considerable success to the data of the specific heat and the NMR spin-lattice-relaxation rate of CeRu$_4$Sn$_6$ and found the field dependence of these properties to be fully reconcilable in the framework of this model. The temperature evolution of electronic and thermodynamic properties is driven by two nested energy gaps, $\Delta E_{g1} = 30$ K and $\Delta E_{g2} \approx 0.65$ K (at zero field), centered on the Fermi energy. The gapping is not complete and a residual number of heavy-mass charge carriers within the smaller of the two gaps achieves a finite electrical conductivity even at the lowest temperatures. These states are correlated, presumably due to the Kondo-screening effect, as inferred from strong temperature dependences of the Sommerfeld coefficient of the $4f$ increment to the specific heat and the magnetic susceptibility, both of which are found to saturate at large values as $T \to 0$.

The scope of the physics forwarded for CeRu$_4$Sn$_6$ in this work provides a platform from which to test the predicted nodal Kondo insulating state as a new type of semimetal that forms under favorable conditions.[33] The axial symmetry of nodes of vanishing density of states sets the stage for anisotropic electronic conduction. Anisotropic magnetic properties in CeRu$_4$Sn$_6$ single crystals have recently been reported.[34] A considerable magnetocrystalline anisotropy is evident between the basal plane and the tetragonal c axis. In particular, a tiny c-axis magnetization of 0.065 μ_B at 3 K was found in 6 T which amounts to no more than about 20% of the moment extracted along the isotropic basal plane directions. Furthermore, our results may well reflect the interplay between Ruderman-Kittel-Kasuya-Yoshida and Kondo interaction in the limit of a very low carrier concentration as discussed by Coqblin *et al.*[35]

Future studies on CeRu$_4$Sn$_6$ would benefit from magnetic susceptibility data at very low temperatures to assess, for instance, the role of magnetic correlations through progression of the Sommerfeld-Wilson ratio. Electrical-resistivity studies on single crystals are highly desirable and high-resolution inelastic neutron-scattering measurements would conceivably enhance our knowledge about the low-lying spin excitations in the material.

*bruening@cpfs.mpg.de

[1] M. Jaime, R. Movshovich, G. R. Stewart, W. P. Beyermann, M. G. Berisso, M. F. Hundley, P. C. Canfield, and J. L. Sarrao, Nature (London) **405**, 160 (2000).

[2] G. Aeppli and Z. Fisk, Comments Condens. Matter Phys. **16**, 155 (1992).

[3] P. Riseborough, Adv. Phys. **49**, 257 (2000).

[4] S. Gabáni, E. Bauer, S. Berger, K. Flachbart, Y. Paderno, C. Paul, V. Pavlík, and N. Shitsevalova, Phys. Rev. B **67**, 172406 (2003).

[5] A. Strydom, Z. Guo, S. Paschen, R. Viennois, and F. Steglich, Physica B **359-361**, 293 (2005).

[6] I. Das and E. V. Sampathkumaran, Phys. Rev. B **46**, 4250 (1992).

[7] A. Strydom, A. Hillier, D. Adroja, S. Paschen, and F. Steglich, J. Magn. Magn. Mater. **310**, 377 (2007).

[8] R. Pöttgen, R.-D. Hoffmann, E. Sampathkumaran, I. Das, B. Mosel, and R. Müllmann, J. Solid State Chem. **134**, 326 (1997).

[9] N. Koch and A. Strydom, J. Magn. Magn. Mater. **320**, e128 (2008).

[10] E. Brüning, M. Baenitz, A. Gippius, A. Strydom, F. Steglich, and R. Walstedt, J. Magn. Magn. Mater. **310**, 393 (2007).

[11] D. T. Adroja and A. Strydom, ISIS Pulsed Neutron & Muon Source Technical Report, 2006 (unpublished).

[12] F. Blatt, *Thermoelectric Power of Metals* (Plenum Press, New York, 1976).

[13] Z. Guo, M.S. thesis, University of Johannesburg, 2005.

[14] V. Zlatić, R. Monnier, J. K. Freericks, and K. W. Becker, Phys. Rev. B **76**, 085122 (2007).

[15] H. Wilhelm, T. Lühmann, T. Rus, and F. Steglich, Rev. Sci. Instrum. **75**, 2700 (2004).

[16] A. Abragam and B. Bleaney, *Electron Paramagnetic Resonance of Transition Ions* (Oxford University Press, New York, 1970).

[17] A. Strydom and D. Adroja, private communication.

[18] A. Ślebarski, K. Grube, R. Lortz, C. Meingast, and H. v. Löhneysen, J. Magn. Magn. Mater. **272-276**, 234 (2004).

[19] M. Kyogaku, Y. Kitaoka, H. Nakamura, K. Asayama, T. Takabatake, F. Teshima, and H. Fujii, J. Phys. Soc. Jpn. **59**, 1728

(1990).

[20] K. I. Nakamura, Y. Kitaoka, K. Asayama, T. Takabatake, G. Nakamoto, H. Tanaka, and H. Fujii, Phys. Rev. B **53**, 6385 (1996).

[21] A. P. Reyes, R. H. Heffner, P. C. Canfield, J. D. Thompson, and Z. Fisk, Phys. Rev. B **49**, 16321 (1994).

[22] T. Caldwell, A. P. Reyes, W. G. Moulton, P. L. Kuhns, M. J. R. Hoch, P. Schlottmann, and Z. Fisk, Phys. Rev. B **75**, 075106 (2007).

[23] A. K. Rajarajan, A. Rabis, M. Baenitz, A. A. Gippius, E. N. Morozowa, J. A. Mydosh, and F. Steglich, Phys. Rev. B **76**, 024424 (2007).

[24] G. Carter, L. Bennett, and D. Kahan, Prog. Mater. Sci. **20**, 1 (1977).

[25] T. Fukuhara, I. Sakamoto, H. Sato, S. Takayanagi, and N. Wada, J. Phys.: Condens. Matter **1**, 7487 (1989).

[26] S. Takayanagi, T. Fukuhara, H. Sato, N. Wada, and Y. Yamada, Physica B **165-166**, 447 (1990).

[27] D. A. Levitt and R. E. Walstedt, Phys. Rev. Lett. **38**, 178 (1977).

[28] A. Gippius, K. Okhotnikov, M. Baenitz, and A. Shevelkov, Solid State Phenom. **152-153**, 287 (2009).

[29] A. Menth, E. Buehler, and T. H. Geballe, Phys. Rev. Lett. **22**, 295 (1969).

[30] E. Ehrenfreund and L. S. Smith, Phys. Rev. B **16**, 1870 (1977).

[31] E. S. R. Gopal, *Specific Heat at Low Temperatures* (Heywood, London, 1966).

[32] T. A. Costi, Phys. Rev. Lett. **85**, 1504 (2000).

[33] J. Moreno and P. Coleman, Phys. Rev. Lett. **84**, 342 (2000).

[34] S. Paschen, H. Winkler, T. Nezu, M. Kriegisch, G. Hilscher, J. Custers, A. Prokofiev, and A. Strydom, J. Phys.: Conf. Ser. **200**, 012156 (2010).

[35] B. Coqblin, C. Lacroix, M. A. Gusmao, and J. R. Iglesias, Phys. Rev. B **67**, 064417 (2003).